Inorg. Chem. **1992**, *31*, 1173–1181 **1173**

Contribution from the Biomedical Chemistry Research Center, Department of Chemistry, University of Cincinnati, Cincinnati, Ohio 45221-0172, and Department of Chemistry, Wayne State University, Detroit, Michigan 48202-3929

Thiolato–Technetium Complexes. 5.[1] Synthesis, Characterization, and Electrochemical Properties of Bis(*o*-phenylenebis(dimethylarsine))technetium(II) and -technetium(III) Complexes with Thiolato Ligands. Single-Crystal Structural Analyses of *trans*-$[Tc(SCH_3)_2(DIARS)_2]PF_6$ and *trans*-$[Tc(SC_6H_5)_2(DIARS)_2]^0$

Takumi Konno,[2,3] Mary Jane Heeg,[4] Jeanne A. Stuckey,[4] Jon R. Kirchhoff,[5] William R. Heineman,[2]
and Edward Deutsch*,[2]

Received July 24, 1991

Three different thiols have been brought into reaction with *trans*-$[Tc(OH)(O)(DIARS)_2]^{2+}$ to produce initially the Tc(II) complex, $[Tc(SR)_2(DIARS)_2]^0$, which can be oxidized to the Tc(III) complex, $[Tc(SR)_2(DIARS)_2]^+$ (DIARS = *o*-phenylenebis(dimethylarsine)). In the case of SR = SCH_3 and $SCH_2C_6H_5$, the Tc(II) and Tc(III) products were found to be in the trans geometry, while for SR = SC_6H_5, both cis and trans isomers were generated. Two of the complexes were structurally characterized by X-ray diffraction. *trans*-$[Tc(SCH_3)_2(DIARS)_2]PF_6$, chemical formula $TcAs_4S_2PF_6C_{22}H_{38}$, crystallizes in the monoclinic space group $C2/c$, with $Z = 4$ and lattice parameters $a = 20.440$ (3) Å, $b = 11.989$ (2) Å, $c = 13.284$ (2) Å, $\beta = 98.24$ (1)°, and $V = 3221.5$ (7) Å^3. The final weighted R value is 0.026. The Tc atom occupies an inversion center. Important molecular parameters are Tc^{III}–S = 2.292 (2) Å, Tc^{III}–As = 2.496 (2) Å, S–C = 1.816 (7) Å, and Tc–S–C = 118.9 (2)°. *trans*-$[Tc(SC_6H_5)_2(DIARS)_2]^0$, chemical formula $TcAs_4S_2C_{32}H_{42}$, crystallizes in the monoclinic space group $P2_1/c$ with $Z = 2$ and lattice parameters $a = 12.406$ (2) Å, $b = 14.924$ (3) Å, $c = 9.848$ (2) Å, $\beta = 108.62$ (2)°, and $V = 1727.9$ (6) Å^3. The final weighted R value is 0.027. The Tc atom occupies an inversion center. Important molecular parameters are Tc^{II}–S = 2.410 (2) Å, Tc^{II}–As = 2.471 (2) Å, S–C = 1.794 (7) Å, and Tc–S–C = 119.5 (3)°. Representative elemental analyses, FAB mass spectra, and visible–UV spectra are reported. Electrochemical and spectroelectrochemical measurements were taken on *trans*-$[Tc(SCH_3)_2(DIARS)_2]^+$, *trans*-$[Tc(SCH_2C_6H_5)_2(DIARS)_2]^+$, and *cis*-$[Tc(SC_6H_5)_2(DIARS)_2]^+$, which exhibit a reversible Tc(III/II) redox couple in the range −0.32 to −0.47 V vs. Ag/AgCl. Another redox couple is present in the range −1.22 to −1.70 V; this is ascribed to Tc(II/I) and is reversible only for SR = $SCH_2C_6H_5$ at 20 °C. At room temperature, chemically irreversible couples are exhibited at ca. +1.0 V for Tc(IV/III).

Introduction

In the first four articles of this series, we have reported and characterized technetium–thiolato complexes of tertiary diphosphine ligands (D) of the form $[Tc(SR)_2D_2]^{0/+}$ wherein SR is an alkane-, phenylmethane-, or arenethiolate. We now investigate analogous thiolato–Tc complexes wherein D is an arsine ligand. In 1959, Fergusson and Nyholm[6] reported the first DIARS complexes of technetium, $[TcD_2X_2]^+$ (X = Cl, Br, I), along with the (then) new oxidation states of Tc(II) and Tc(III). Since that time, the chemistry of Tc(II) and Tc(III) has expanded explosively[7] but the chemistry of Tc–DIARS complexes continues to be dominated by halo complexes. Most main-block transition elements form stable complexes with DIARS, although only the dihalide and pseudohalide complexes with Tc have been well characterized up to now. Our previous studies have included a comparison of the redox chemistry of $[TcX_2D_2]^+$ complexes, and it was seen that, for X = halides, the Tc^{III} complexes with D = DIARS were easier to reduce to Tc^{II} than were those with D = DMPE, by about 100–150 mV.[8] It was also observed that the bis(thiolato)–Tc^{III} complexes $[Tc(SR)_2(DMPE)_2]^+$ were much more resistant to reduction to Tc^{II} than their dihalo $[TcX_2(DMPE)_2]^+$ analogues.[1] It is our thinking that DIARS–thiolato–technetium complexes might bridge the potential range between the easily reduced $[TcX_2(DIARS)_2]^+$ complexes and the more difficult to reduce $[Tc(SR)_2(DMPE)_2]^+$ complexes. Substitution on the thiolato R group can afford subtle redox and solubility control. Therefore the present article represents our continuing investigations and reports results on the preparation, characterization, and redox behavior of several $[Tc(SR)_2(DIARS)_2]^{+/0}$ complexes, complementary to our earlier studies on $[Tc(SR)_2(DMPE)_2]^{+/0}$ analogues. There is an ultimate biological interest in these complexes wherein the control of lipophilicity and redox potential is important in drug design.[9]

Acronyms and Abbreviations. The following acronyms and abbreviations are used in this article: DEPE = 1,2-bis(diethylphosphino)ethane; DIARS = *o*-phenylenebis(dimethylarsine); DMF = *N*,*N*-dimethylformamide; DMPE = 1,2-bis(dimethylphosphino)ethane; FAB = fast atom bombardment; OTTLE = optically transparent thin-layer electrode; PDE = platinum disk electrode; Ph = phenyl; STTCT = sulfur-to-technetium charge transfer; TEAP = tetraethylammonium perchlorate.

Experimental Section

Caution. Technetium-99 emits a low-energy (0.292 MeV) β particle with a half-life of 2.12×10^5 yr. When handled in milligram amounts, ^{99}Tc does not present a serious health hazard, since common laboratory materials provide adequate shielding. Bremsstrahlung is not a significant problem due to the low energy of the β-particle emission, but normal radiation safety procedures must be used at all times, especially when solid samples are handled, to prevent contamination and inadvertent inhalation. In this paper, the symbol Tc refers only to technetium-99; the metastable isotope ^{99m}Tc was not used in these studies.

Reagents. Unless otherwise noted, all chemicals were of reagent grade. The DIARS ligand was purchased from Strem Chemical Co. and used without further purification. The magic bullet matrix (a 5:1 mixture of dithiothreitol and dithioerythritol in a small amount of methanol) was used in measurements of the FAB mass spectra. DMF from Burdick and Jackson and polarographic grade TEAP from G. F. Smith Chemicals were used in the electrochemical measurements. Prior to use, the TEAP was dried at 60 °C in vacuo over P_2O_5. No significant electroactive impurities were detected in either the solvent or supporting electrolyte.

Syntheses. ***trans*-$[Tc(OH)(O)(DIARS)_2](PF_6)_2$.** To a solution containing 100 mg of NH_4TcO_4 in 15 mL of degassed 95% methanol was added 0.8 g of neat DIARS (2.8×10^{-3} mol), followed by 0.4 mL of concentrated CF_3SO_3H. The solution was stirred at 60 °C for 20 min

---

(1) (a) Part 1: Konno, T.; Heeg, M. J.; Deutsch, E. *Inorg. Chem.* **1988**, *27*, 4113–4121. (b) Part 2: Konno, T.; Kirchhoff, J. R.; Heineman, W. R.; Deutsch, E. *Inorg. Chem.* **1989**, *28*, 1174–1179. (c) Part 3: Konno, T.; Heeg, M. J.; Deutsch, E. *Inorg. Chem.* **1989**, *28*, 1694–1700. (d) Part 4: Konno, T.; Heeg, M. J.; Seeber, R.; Kirchhoff, J. R.; Heineman, W. R.; Deutsch, E. *Transition Met. Chem.*, in press.

(2) University of Cincinnati.

(3) On leave from the Department of Chemistry, The University of Tsukuba, Tsukuba, Ibaraki 305, Japan.

(4) Wayne State University.

(5) Present address: Department of Chemistry, University of Toledo, Toledo, OH 43606.

(6) Fergusson, J. E.; Nyholm, R. S. *Nature* **1959**, *183*, 1039–1040.

(7) Technetium chemistry reviews: Bandoli, G.; Mazzi, U.; Roncari, E.; Deutsch, E. *Coord. Chem. Rev.* **1982**, *44*, 191–227. Deutsch, E.; Libson, K.; Jurisson, S.; Lindoy, L. F. *Prog. Inorg. Chem.* **1983**, *30*, 75–139. Melnik, M.; Van Lier, J. E. *Coord. Chem. Rev.* **1987**, *77*, 275–324.

(8) Ichimura, A.; Heineman, W. R.; Vanderheyden, J.-L.; Deutsch, E. *Inorg. Chem.* **1984**, *23*, 1272–1278.

(9) Reviews of technetium complexes as radiopharmaceuticals: Deutsch, E.; Libson, K. *Comments Inorg. Chem.* **1984**, *3*, 83–103. Clarke, M. J.; Podbielski, L. *Coord. Chem. Rev.* **1987**, *78*, 253–331.

under an argon atmosphere while the solution turned dark yellow-orange. Addition of 2 g of NH_4PF_6 in a small amount of water followed by cooling in a refrigerator for 1 day produced a dark yellow precipitate of *trans*-$[Tc(OH)(O)(DIARS)_2](PF_6)_2$. Yield: 400 mg (73%).

***trans*-$[Tc(SCH_3)_2(DIARS)_2]PF_6$.** The *trans*-$[Tc(SCH_3)_2(DIARS)_2]PF_6$ complex was prepared by a method similar to that employed for *trans*-$[Tc(SCH_3)_2(DMPE)_2]PF_6$,[1a] using *trans*-$[Tc(OH)(O)(DIARS)_2](PF_6)_2$ instead of *trans*-$[Tc(OH)(O)(DMPE)_2](PF_6)_2$ as the starting material. To a suspension containing 100 mg of *trans*-$[Tc(OH)(O)(DIARS)_2](PF_6)_2$ (1.0×10^{-4} mol) in 20 mL of degassed ethanol was added 70 mg of $NaSCH_3$ (1.0×10^{-3} mol) in 5 mL of degassed ethanol. The mixture was stirred at 60 °C for 30 min under an argon atmosphere, whereupon the solution became deep purple. To this was added 0.5 mL of saturated NH_4PF_6 in water, and the solution turned blue almost immediately. After the blue reaction solution (ethanol solvent) was cooled in a refrigerator for 2 days, the resultant crystals of *trans*-$[Tc(SCH_3)_2(DIARS)_2]PF_6$ were collected by filtration. Yield: 40 mg (44%). Crystals suitable for X-ray structural studies were obtained by allowing the blue reaction solution to stand at room temperature for several days.

***trans*-$[Tc(SCH_2C_6H_5)_2(DIARS)_2]PF_6$.** This complex was prepared by a method similar to that employed for *trans*-$[Tc(SCH_2C_6H_5)_2(DMPE)_2]PF_6$,[1b] using *trans*-$[Tc(OH)(O)(DIARS)_2](PF_6)_2$ instead of *trans*-$[Tc(OH)(O)(DMPE)_2](PF_6)_2$ as the starting material. To a suspension containing 100 mg of *trans*-$[Tc(OH)(O)(DIARS)_2](PF_6)_2$ (1.0×10^{-4} mol) in 20 mL of degassed ethanol was added 0.18 mL of neat $HSCH_2C_6H_5$ (1.5×10^{-3} mol), followed by 0.3 mL of 1 M NaOH. The mixture was stirred at 60 °C for 20 min under an argon atmosphere, whereupon the solution became deep red and deposited a red precipitate. The visible spectrum of the red complex in degassed CH_3CN confirmed that this was *trans*-$[Tc^{II}(SCH_2C_6H_5)_2(DIARS)_2]^0$ (λ_{max}, nm: 536, 456), though this complex decomposed quickly in solution. This complex was also unstable in the solid state and completely decomposed in a few days, forming a dark yellow-brown species which could not be identified. When 1.0 mL of a saturated NH_4PF_6 solution was added to the red reaction solution containing a red precipitate, the solution turned deep blue and a blue precipitate appeared. After the addition of a small amount of CH_3CN to dissolve the blue precipitate, the blue reaction mixture was cooled in a refrigerator overnight and then the resultant blue crystals of *trans*-$[Tc(SCH_2C_6H_5)_2(DIARS)_2]PF_6$ were collected by filtration. Yield: 40 mg (35%). Anal. Calcd for $[Tc(SCH_2C_6H_5)_2(DIARS)_2]PF_6 = C_{34}H_{46}F_6PS_2As_4Tc$: C, 38.44; H, 4.36; F, 10.73; S, 6.03. Found: C, 38.47; H, 4.40; F, 10.49; S, 6.79.

***trans*-$[Tc(SC_6H_5)_2(DIARS)_2]$.** To a suspension containing 100 mg of *trans*-$[Tc(OH)(O)(DIARS)_2](PF_6)_2$ (1.0×10^{-4} mol) in 20 mL of degassed ethanol was added 0.3 mL of neat HSC_6H_5 (2.9×10^{-3} mol), followed by 0.6 mL of 1 M NaOH. The mixture was stirred at 60 °C for 20 min under an argon atmosphere, whereupon the solution became almost black. As the black solution was cooled to room temperature, a small amount of blue-purple precipitate of *trans*-$[Tc^{II}(SC_6H_5)_2(DIARS)_2]^0$ appeared and was collected by filtration. Yield: 10 mg (11%). The crystals of this complex used for X-ray structural analysis were obtained by recrystallization from CH_2Cl_2 in a refrigerator. It was found from visible spectral measurements and oxidation to the corresponding Tc^{III} species that the remaining dark green filtrate contained *cis*-$[Tc^{II}(SC_6H_5)_2(DIARS)_2]^0$, though the isolation of this cis Tc^{II} complex was unsuccessful (λ_{max}, nm: 597, 491, 391 sh).

***cis*-$[Tc(SC_6H_5)_2(DIARS)_2]PF_6$.** To the dark green filtrate of *cis*-$[Tc(SC_6H_5)_2(DIARS)_2]^0$ obtained above was added 1.5 mL of saturated NH_4PF_6. The mixture was stirred at 50 °C for 20 min in the presence of air, whereupon the solution turned dark blue and a blue precipitate appeared. After the addition of a small amount of CH_3CN to dissolve the blue precipitate, the dark blue reaction solution was kept in the refrigerator for 3 days and the resultant crystals of *cis*-$[Tc(SC_6H_5)_2(DIARS)_2]PF_6$ were collected by filtration. Yield: 20 mg (19%). Anal. Calcd for $[Tc(SC_6H_5)_2(DIARS)_2]PF_6 = C_{32}H_{42}F_6PS_2As_4Tc$: C, 37.15; H, 4.09; F, 11.02. Found: C, 36.41; H, 4.09; F, 10.65.

***trans*-$[Tc(SC_6H_5)_2(DIARS)_2]PF_6$.** To a suspension of 30 mg of *trans*-$[Tc^{II}(SC_6H_5)_2(DIARS)_2]^0$ in 5 mL of acetone was added 200 mg of NH_4PF_6 in a small amount of water, followed by one drop of 30% H_2O_2 and one drop of concentrated HPF_6. After the mixture was stirred at room temperature for 1 h, the resultant green-blue product of *trans*-$[Tc^{III}(SC_6H_5)_2(DIARS)_2]PF_6$ was collected by filtration and then recrystallized from acetone–ethanol in the refrigerator. Yield: 35 mg (72%). λ_{max}, nm (acetone): 699, 393. The green-blue crystalline material was contaminated with a small amount of *cis*-$[Tc(SC_6H_5)_2(DIARS)_2]PF_6$. Further recrystallization of this product increased the amount of *cis*-$[Tc(SC_6H_5)_2(DIARS)_2]PF_6$.

Reduction of Complexes. To anaerobic solutions of *trans*-$[Tc^{III}(SCH_3)_2(DIARS)_2]PF_6$, *trans*-$[Tc^{III}(SCH_2C_6H_5)_2(DIARS)_2]PF_6$, *trans*-$[Tc^{III}(SC_6H_5)_2(DIARS)_2]PF_6$, and *cis*-$[Tc^{III}(SC_6H_5)_2(DIARS)_2]PF_6$ in acetonitrile were added a few drops of $(C_4H_9)_4NBH_4$ in a small amount of ethanol under an argon atmosphere. These solutions rapidly turned purple, red-purple, blue-purple, and dark green, respectively. Their visible–UV spectra were then the same as those of *trans*-$[Tc^{II}(SCH_3)_2(DIARS)_2]^0$, *trans*-$[Tc^{II}(SCH_2C_6H_5)_2(DIARS)_2]^0$, *trans*-$[Tc^{II}(SC_6H_5)_2(DIARS)_2]^0$, and *cis*-$[Tc(SC_6H_5)_2(DIARS)_2]^0$, respectively. The same color changes were generated by adding $NaSCH_3$ to *trans*-$[Tc^{III}(SCH_3)_2(DIARS)_2]PF_6$, $HSCH_2C_6H_5$ to *trans*-$[Tc^{III}(SCH_2C_6H_5)_2(DIARS)_2]PF_6$, and HSC_6H_5 to *trans*- and *cis*-$[Tc(SC_6H_5)_2(DIARS)_2]PF_6$, followed by a small amount of 1 M NaOH. This behavior is analogous to that observed with *trans*-$[Tc^{III}(SR)_2(D)_2]PF_6$ (D = DMPE, DEPE) complexes.[1a,b]

Measurements. Elemental analyses were performed by Galbraith Laboratories, Knoxville, TN. Visible–UV spectra were recorded in acetonitrile or dichloromethane on a Cary 210 spectrophotometer (Varian) at ambient temperatures. FAB mass spectra were recorded using the magic bullet matrix on a VG 30-250 spectrometer (VG Instruments, Inc.) at the probe temperature. Xenon was used as the primary beam gas, and the ion gun was operated at 8 keV and 100 μA. Data were collected generally over the mass range 100–1000 Da at 0.7 s/scan. Electrochemical measurements were made with a Bioanalytical Systems (BAS) CV-1B voltammograph. Potentials were monitored with a Keithley 178 digital multimeter, and voltammograms were recorded on a Hewlett Packard 7015B X-Y recorder. Visible spectra in the spectroelectrochemical experiment were recorded on a Cary 210 spectrophotometer; the cell compartment was modified to accommodate electrical leads and an inert-gas inlet. The working electrode for conventional cyclic voltammetry was a PDE (BAS). OTTLE's were constructed as previously described with a 100 wire/in. gold minigrid.[10] An aqueous Ag/AgCl (3 M NaCl) electrode (BAS) and a platinum wire were used as reference and auxiliary electrodes, respectively. The reference electrode was isolated from the solution by a porous Vycor plug. All potentials are reported vs the Ag/AgCl (3 M NaCl) electrode. In general, electrochemical experiments were performed as previously described.[1b,8,11] Each spectrum in the spectropotentiostatic experiments was recorded 5 min after potential application. This time was sufficient to attain equilibrium values of [O]/[R].

Crystallography. Single-crystal X-ray diffraction experiments were performed on a Nicolet R3 automated diffractometer with Mo Kα radiation (λ = 0.71073 Å) and a graphite monochromator at ambient temperature. Details of data collection in common were as follows: scan method $\theta/2\theta$, scan rate variable 2–5°/min, ratio of background to scan time 0.5, 2θ range 6–52°. Both structures were solved by Patterson methods and refined in a full matrix with the programs of SHELX-76.[12] All non-hydrogen atoms were refined anisotropically. Hydrogen atoms were placed in a combination of observed and calculated positions and held invariant. Isotropic temperature factors for the hydrogen atoms were assigned to be equal and refined as a single variable in each structure. Absorption corrections were made by empirical methods.[13] One reflection [120] was removed from the data of *trans*-$[Tc(SC_6H_5)_2(DIARS)_2]$ due to secondary extinction. Neutral-atom scattering factors and corrections for anomalous dispersion were from ref 14. Table I contains further crystallographic data.

Results

Synthesis and Characterization. Tc–DIARS compounds with the thiolato ligands $-SCH_3$, $-SCH_2C_6H_5$, and $-SC_6H_5$ have been prepared. In all cases, 10 times excess thiol is added to a suspension of Tc(V) starting material, $[Tc(OH)(O)(DIARS)_2]^{2+}$. The initial product of this reduction/substitution reaction is the thiolato–Tc(II)–DIARS complex, which is subsequently oxidized to the Tc(III) complex.

In the reaction utilizing $NaSCH_3$, the first product consists of a deep purple solution of *trans*-$[Tc^{II}(SCH_3)_2(DIARS)_2]^0$. Because this complex in solution is unstable in the presence of air and subject to decomposition and oxidation reactions, it was not isolated. Acid oxidation of this purple reaction solution produces the trans Tc(III) complex, *trans*-$[Tc(SCH_3)_2(DIARS)_2]^+$, which

---

[10] DeAngelis, T. P.; Heineman, W. R. *J. Chem. Educ.* **1976**, *53*, 594–597.

[11] Rohrbach, D. F.; Heineman, W. R.; Deutsch, E. *Inorg. Chem.* **1979**, *18*, 2536–2542.

[12] Sheldrick, G. M. SHELX-76. University Chemical Laboratory, Cambridge, England, 1976.

[13] Sheldrick, G. M. SHELXTL. University of Gottingen, Germany, 1978.

[14] *International Tables for X-ray Crystallography*; Kynoch Press: Birmingham, England, 1974; Vol. 4 (present distributor D. Reidel, Dordrecht, The Netherlands).

Table I. Experimental Crystallographic Data[a] for *trans*-$[Tc(SCH_3)_2(DIARS)_2]PF_6$ (**1**) and *trans*-$[Tc(SC_6H_5)_2(DIARS)_2]$ (**2**)

	1	**2**
formula	$TcAs_4S_2PF_6C_{22}H_{38}$	$TcAs_4S_2C_{32}H_{42}$
mol wt	910.23	889.41
space group	$C2/c$ (No. 15)	$P2_1/c$ (No. 14)
cell dimens[b]		
a, Å	20.440 (3)	12.406 (2)
b, Å	11.989 (2)	14.924 (3)
c, Å	13.284 (2)	9.848 (2)
β, deg	98.24 (1)	108.62 (2)
V, Å^3	3221.5 (7)	1727.9 (6)
Z	4	2
density (calc), g cm^{-3}	1.876	1.709
μ (cm^{-1})	47.3	43.4
transm coeff	0.270–0.200	0.527–0.367
R, R_w	0.035, 0.026	0.043, 0.027

[a] $T = 20$ °C; $\lambda = 0.71073$ Å; $R = (\sum|\Delta F|)/\sum|F_o|$; $R_w = [(\sum w|\Delta F|^2)/\sum wF_o^2]^{1/2}$. [b] Lattice parameters from 25 high-angle reflections constrained to be monoclinic.

is characteristically deep blue. Confirmation of this compositional assignment was made crystallographically. Its positive-ion FAB mass spectrum shows the parent peak at m/z 765, corresponding to $[Tc(SCH_3)_2(DIARS)_2]^+$. Other fragments listed in Table II reflect the loss of SR and R groups. Visible–UV absorptions for *trans*-$[Tc(SCH_3)_2(DIARS)_2]^+$ are presented in Table III.

In the reaction of the thiol $HSCH_2C_6H_5$ with Tc(V), the initial products are a red solution and red precipitate of *trans*-$[Tc^{II}(SCH_2C_6H_5)_2(DIARS)_2]^0$. This Tc(II) product, like the methanethiolato complex above, is unstable in air and decomposes both in solution and as a solid. The characterization of this red complex by elemental analysis and FAB mass spectrometry is unsuccessful because of its high air sensitivity. However the assignment of *trans*-$[Tc(SCH_2C_6H_5)_2(DIARS)_2]^0$ is substantiated because (1) the trans Tc(III) isomer, *trans*-$[Tc^{III}(SCH_2C_6H_5)_2(DIARS)_2]^+$, is formed by the oxidation of this red complex and (2) reduction of *trans*-$[Tc^{III}(SCH_2C_6H_5)_2(DIARS)_2]^+$ by chemical or electrochemical methods yields this red complex. Acid oxidation of this red reaction solution yields the deep blue complex *trans*-$[Tc^{III}(SCH_2C_6H_5)_2(DIARS)_2]^+$. The elemental analysis of this complex as the PF_6^- salt gives results consistent with the proposed formulation. Its positive-ion FAB mass spectrum shows the expected m/z for the M^+ parent ion at 917, and other lighter masses can be identified as corresponding to losses of R and/or SR groups from the parent ion (Table II). Visible–UV spectral properties of *trans*-$[Tc^{III}(SCH_2C_6H_5)_2(DIARS)_2]^+$ are listed in Table III. Its visible–UV absorption spectrum is quite similar to that of *trans*-$[Tc^{III}(SCH_3)_2(DIARS)_2]^+$ (Figure 1), the structure of which was determined by a crystallographic analysis. Accordingly, the DIARS–Tc(III) complex with phenylmethanethiolate, $[Tc(SCH_2C_6H_5)_2(DIARS)_2]^+$, can be assigned trans geometry.

The reaction of Tc^V with the arenethiol HSC_6H_5 is more complicated. The initial product solution consists of two isomers of the Tc(II) complex: a blue-purple precipitate of *trans*-$[Tc^{II}(SC_6H_5)_2(DIARS)_2]^0$ and a green solution containing *cis*-$[Tc^{II}(SC_6H_5)_2(DIARS)_2]^0$. The geometry and compositional assignment of the blue-purple trans product have been confirmed by crystallography. Its positive-ion FAB mass spectrum shows the parent ion at m/z 889 and other reasonable fragment ions (Table II). The visible–UV data for *trans*-$[Tc^{II}(SC_6H_5)_2(DIARS)_2]^0$ are listed in Table III. Oxidation of this trans Tc(II) product with H_2O_2 yields a green-blue solution which contains mostly *trans*-$[Tc^{III}(SC_6H_5)_2(DIARS)_2]^+$ but is also contaminated with the analogous cis isomer. Isomerization to the cis isomer continues throughout recrystallizations, demonstrating that cis is the favored geometry. Isomerization to the cis Tc(III) form can be followed by observing the decreasing intensity of the main visible band of the trans Tc(III) complex at 699 nm and the concomitant increase at ca. 580 nm, which is the main band for the cis Tc(III) isomer. No spectral change with time is noted for the cis Tc(III) isomer in solution. The trans Tc(III) product is characterized by its FAB mass spectrum (Table II), and its visible–UV λ_{max} values are listed in the Experimental Section. The Tc(II) product, *cis*-$[Tc(SC_6H_5)_2(DIARS)_2]^0$, in the initial dark green solution was not isolated from solution due to its high solubility. However, the visible–UV data for this green solution are given in the Experimental Section, and its similarity to the visible spectrum of *cis*-$[Tc^{II}(SC_6H_4\text{-}p\text{-}Cl)_2(DMPE)_2]^0$, which has been characterized by a single-crystal X-ray analysis,[1c] supports the assignment. Acid oxidation of the green cis Tc(II) solution produces the dark blue cis Tc(III) complex, *cis*-$[Tc(SC_6H_5)_2(DIARS)_2]^+$. Elemental analysis of this product gives results consistent with the proposed formulation. Its FAB mass spectral data and visible–UV spectral data are presented in Tables II and III. The visible spectrum is quite similar to that of the analogous DMPE complex, *cis*-$[Tc(SC_6H_5)_2(DMPE)_2]^+$ (Figure 2), which has been characterized by a single-crystal X-ray analysis.[1d] This supports the assignment of cis geometry for this complex. Reduction of any of these Tc(III) complexes produces the analogous Tc(II) complexes, and this reversible redox behavior further supports the assignments.

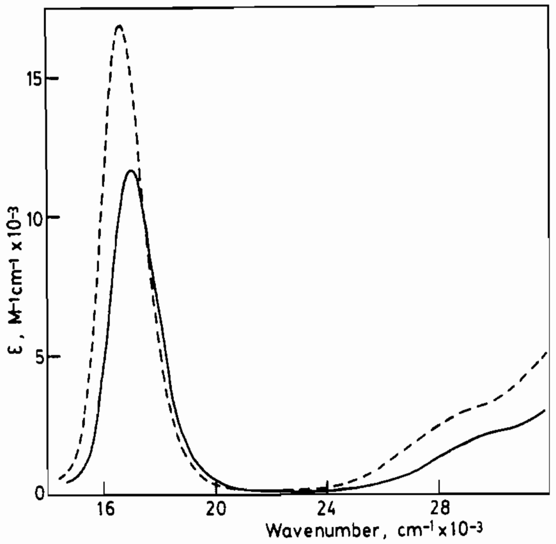

Figure 1. Visible spectra of *trans*-$[Tc(SCH_3)_2(DIARS)_2]^+$ (—) and *trans*-$[Tc(SCH_2C_6H_5)_2(DIARS)_2]^+$ (---) recorded in CH_3CN.

Crystal Structure of *trans*-$[Tc^{III}(SCH_3)_2(DIARS)_2]PF_6$ (1). Figure 3 illustrates the molecular geometry and labeling scheme for the cation. Fractional atomic coordinates are listed in Table IV. Selected bond lengths and angles are presented in Table V. The central technetium atom occupies a crystallographic inversion center. The ligand arrangement is roughly octahedral, with the

Table II. Mass Spectral Data for $[Tc(SR)_2(DIARS)_2]^{+/0}$ Complexes

		m/z					
	complex	fragment ions, M – ( )					
complex	ion, M^+	(R)	(SR)	(2R)	(R,SR)	(DIARS)	(2R,DIARS)
trans-$[Tc(SCH_3)_2(DIARS)_2]^+$	765[a]		717		703		449
trans-$[Tc(SCH_2C_6H_5)_2(DIARS)_2]^+$	917	826	793	735	703		449[a]
trans-$[Tc(SC_6H_5)_2(DIARS)_2]^+$	889[a]		780			603	449
cis-$[Tc(SC_6H_5)_2(DIARS)_2]^+$	889[a]		780			603	449
trans-$[Tc(SC_6H_5)_2(DIARS)_2]^0$	889[a]		780			603	448

[a] Most intense peak in the spectrum.

Table III. Visible–UV Spectral Data for $[Tc(SR)_2(DIARS)_2]^{+/0}$ Complexes[a]

complex	$\nu_{max}/10^3$, cm^{-1}	$\epsilon/10^3$, $M^{-1}\ cm^{-1}$
trans-$[Tc(SCH_3)_2(DIARS)_2]^{+\ b}$	17.01	11.70
	30.67 sh	2.42
	35.21	7.51
	40.65 sh	6.99
trans-$[Tc(SCH_2C_6H_5)_2(DIARS)_2]^{+\ b}$	16.64	16.93
	29.50 sh	3.15
	37.31 sh	12.06
	43.67 sh	41.29
cis-$[Tc(SC_6H_5)_2(DIARS)_2]^{+\ b}$	17.27	10.01
	23.26	4.38
	27.93	5.14
	40.82	30.46
trans-$[Tc(SC_6H_5)_2(DIARS)_2]^{0\ c}$	17.06	9.05
	21.37	1.56
	25.45	4.16
	37.31	25.19

[a] sh denotes a shoulder. [b] Spectra recorded in CH_3CN. [c] Spectrum recorded in CH_2Cl_2.

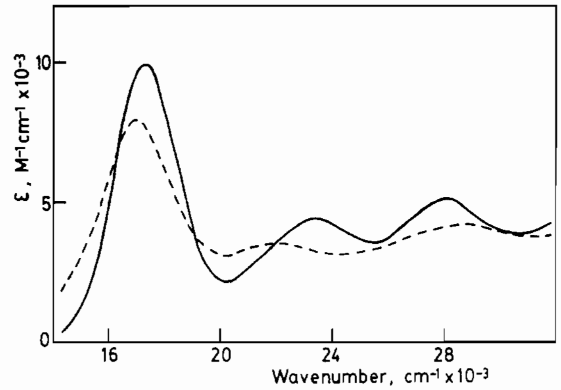

Figure 2. Visible spectra of *cis*-$[Tc(SC_6H_5)_2(DIARS)_2]^+$ (—) and *cis*-$[Tc(SC_6H_5)_2(DMPE)_2]^+$ (---) recorded in CH_3CN.

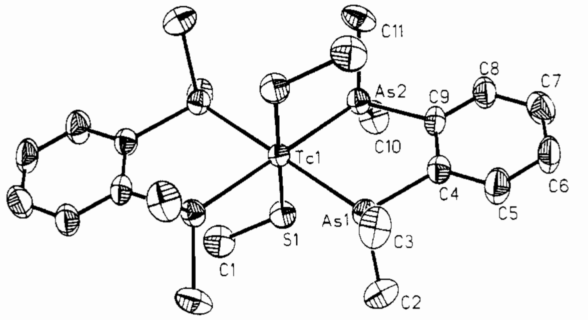

Figure 3. Perspective view of *trans*-$[Tc(SCH_3)_2(DIARS)_2]^+$ showing the assigned labeling. The Tc atom occupies a crystallographic inversion center.

primary distortion being the restricted bite angle of the DIARS chelate (82.39 (2)° for As1–Tc–As2). The monodentate methanethiolato ligands are mutually trans. There are no unusual close contacts between chemical fragments in the lattice. The two independent As atoms along with the central Tc atom define a plane required to include the two symmetry-related As atoms. The S1–Tc vector is nearly orthogonal to this basal plane, making an angle of 87.5 (4)° with it. The aromatic ring portion of the DIARS ligand is planar (RMSD = 0.008 Å), and As1 and As2 occupy this plane (displacements are –0.016 and 0.003 Å, respectively). The Tc atom is slightly displaced from this aromatic ring plane by 0.340 Å. The dihedral angle between the aromatic ring plane and the basal coordinatiaon plane is 10.6 (4)°, which defines a small bend in the DIARS ligand. The torsion angles describing the orientation of the methanethiolato ligands are C1–S1–Tc1–As1 = 134.6 (3)° and C1–S1–Tc1–As2 = –143.0 (3)°.

Table IV. Fractional Atomic Coordinates for *trans*-$[Tc(SCH_3)_2(DIARS)_2]PF_6$

atom	*x*	*y*	*z*
Tc1	0.25000	0.25000	0.00000
As1	0.24030 (3)	0.45761 (5)	–0.00736 (6)
As2	0.36186 (3)	0.39463 (6)	0.09250 (5)
S1	0.21258 (8)	0.2523 (2)	0.1546 (1)
C1	0.1497 (3)	0.1525 (6)	0.1784 (5)
C2	0.1835 (3)	0.5340 (5)	0.0790 (5)
C3	0.2147 (3)	0.5341 (5)	–0.1365 (4)
C4	0.3266 (3)	0.5236 (5)	0.0383 (4)
C5	0.3389 (4)	0.6373 (6)	0.0301 (5)
C6	0.4005 (4)	0.6819 (6)	0.0623 (6)
C7	0.4514 (3)	0.6133 (6)	0.1062 (5)
C8	0.4409 (3)	0.4993 (6)	0.1152 (5)
C9	0.3796 (3)	0.4540 (5)	0.0810 (5)
C10	0.3800 (3)	0.2803 (5)	0.2386 (4)
C11	0.4385 (3)	0.2241 (6)	0.0514 (5)
P1	0.5000	–0.0579 (2)	0.25000
F1	0.4587 (3)	–0.0580 (4)	0.1418 (4)
F2	0.4550 (3)	0.0329 (5)	0.2794 (5)
F3	0.4555 (3)	–0.1468 (5)	0.2803 (5)

Table V. Selected Bond Lengths (Å) and Angles (deg) for *trans*-$[Tc(SCH_3)_2(DIARS)_2]PF_6$

Tc1–As1	2.498 (1)	As1–C4	1.950 (6)
Tc1–As2	2.494 (1)	As2–C9	1.955 (6)
Tc1–S1	2.292 (2)	As2–C10	1.930 (6)
As1–C2	1.971 (7)	As2–C11	1.927 (6)
As1–C3	1.949 (6)	S1–C1	1.816 (7)
Tc1–As1–C2	119.4 (2)	Tc1–As2–C11	119.4 (2)
Tc1–As1–C3	120.9 (2)	Tc1–S1–C1	118.9 (2)
Tc1–As1–C4	109.2 (2)	As1–Tc1–As2	82.39 (2)
Tc1–As2–C9	109.8 (2)	As1–Tc1–S1	89.32 (5)
Tc1–As2–C10	120.4 (2)	As2–Tc1–S1	87.48 (4)

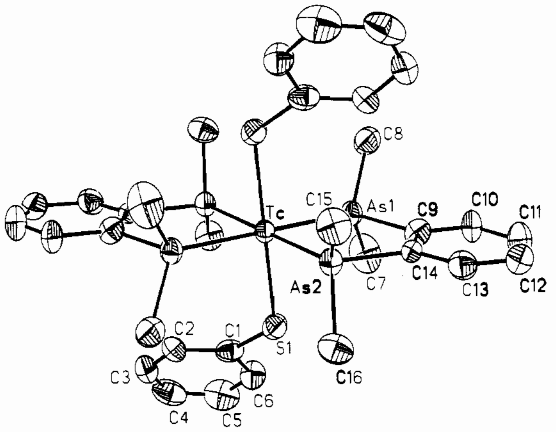

Figure 4. Perspective view of *trans*-$[Tc(SC_6H_5)_2(DIARS)_2]^0$ showing the assigned labeling. The Tc atom occupies a crystallographic inversion center.

The Tc^{III}–As bond lengths average 2.496 (2) Å. The As–C(methyl) distances average 1.94 (2) Å. These methyl groups are bent away from the central Tc atom, showing C–As–Tc bond angles greater than tetrahedral values (119–120°). As–C(ring) lengths average 1.95 (1) Å. The Tc^{III}–S distance is 2.292 (2) Å. Other structural parameters within the thiolato ligand are S–C = 1.816 (7) Å and Tc–S–C = 118.9 (2)°. In the PF_6 anion, phosphorus lies on a crystallographic 2-fold rotation axis. The P–F distances range from 1.559 (4) to 1.494 (5) Å and average 1.52 (3) Å. Cis F–P–F angles range from 87.9 (5)° to 91.6 (4)°.

Crystal Structure of *trans*-$[Tc^{II}(SC_6H_5)_2(DIARS)_2]^0$ (2). Figure 4 illustrates the molecular geometry and adopted labeling scheme of the molecule. Fractional coordinates are given in Table VI. Selected bond lengths and angles are listed in Table VII. The neutral molecule occupies a crystallographic inversion center. There are no ions or solvent molecules present in the lattice. The ligand arrangement is approximately octahedral, subject to the acute bite angle of the DIARS ligand (83.02 (2)° for As1–Tc–

Table VI. Fractional Atomic Coordinates for *trans*-$[Tc(SC_6H_5)_2(DIARS)_2]$

atom	*x*	*y*	*z*
Tc	0.00000	0.50000	0.50000
As1	0.14054 (6)	0.51802 (5)	0.37170 (8)
As2	0.13704 (7)	0.38681 (5)	0.63691 (8)
S1	−0.0762 (2)	0.3765 (1)	0.3408 (2)
C1	−0.2144 (6)	0.3864 (5)	0.2093 (8)
C2	−0.3130 (6)	0.4111 (5)	0.2409 (8)
C3	−0.4158 (6)	0.4135 (6)	0.1337 (9)
C4	−0.4291 (7)	0.3884 (6)	−0.004 (1)
C5	−0.3319 (9)	0.3616 (6)	−0.0350 (9)
C6	−0.2252 (6)	0.3607 (5)	0.0683 (8)
C7	0.0969 (7)	0.4912 (7)	0.1657 (7)
C8	0.2156 (6)	0.6335 (5)	0.3732 (8)
C9	0.2679 (6)	0.4342 (5)	0.4496 (7)
C10	0.3613 (6)	0.4294 (5)	0.3955 (8)
C11	0.4470 (7)	0.3713 (6)	0.4522 (9)
C12	0.4503 (7)	0.3184 (5)	0.565 (1)
C13	0.3587 (7)	0.3232 (5)	0.6259 (9)
C14	0.2683 (5)	0.3812 (5)	0.5650 (7)
C15	0.2099 (6)	0.3883 (5)	0.8462 (7)
C16	0.0952 (6)	0.2592 (5)	0.6186 (7)

Table VII. Selected Bond Lengths (Å) and Angles (deg) for *trans*-$[Tc(SC_6H_5)_2(DIARS)_2]$

Tc–As1	2.4730 (6)	As1–C9	1.968 (7)
Tc–As2	2.4694 (8)	As2–C14	1.974 (6)
Tc–S1	2.410 (2)	As2–C15	1.968 (5)
As1–C7	1.967 (5)	As2–C16	1.967 (7)
As1–C8	1.956 (8)	S1–C1	1.794 (7)
Tc–As1–C7	119.9 (2)	Tc–As2–C16	119.8 (2)
Tc–As1–C8	120.2 (2)	Tc–S1–C1	119.5 (3)
Tc–As1–C9	109.9 (2)	As1–Tc–As2	83.02 (2)
Tc–As2–C14	109.7 (2)	As1–Tc–S1	86.84 (4)
Tc–As2–C15	124.7 (2)	As2–Tc–S1	83.72 (5)

As2). The atoms Tc, As1, and As2 define a basal coordination plane that necessarily includes the symmetry-related atoms As1′ and As2′. The Tc–S vector makes an angle of 83.3 (9)° with this basal coordination plane. The torsion angles describing the orientation of the benzenethiolato ligand are C1–S1–Tc–As1 = −111.4 (2)° and C1–S1–Tc–As2 = 165.3 (2)°. The aromatic ring of the DIARS ligand is planar and regular and is nearly coincident with the basal coordination plane; the dihedral angle between these two planes is 2.0 (6)° (cf. the bent DIARS arrangement of structure **2**).

The Tc^{II}–As bond lengths average 2.471 (2) Å. The As–C(methyl) distances average 1.965 (5) Å. As in structure **1**, the methyl groups are bent away from the central Tc atom, resulting in C–As–C bond angles of 119.8–124.7°. As–C(ring) lengths average 1.97 (1) Å. The Tc^{II}–S distance is 2.410 (2) Å, and S–C(phenyl) = 1.794 (7) Å. The bond angle at sulfur is C1–S1–Tc = 119.5 (3)°. The phenyl group is planar and the sulfur atom is nearly in the plane (displacement of S is −0.09 Å). The dihedral angle between the thiolato–phenyl plane and the basal coordination plane is 126.1 (2)°.

Electrochemistry. The results of electrochemical measurements in 0.5 M TEAP/DMF are summarized in Table VIII. The cyclic voltammograms for all three complexes at a PDE are dominated in the negative potential region by two successive one-electron reductions that are assigned as the reductions of Tc(III) to Tc(II) and Tc(II) to Tc(I).[1b,8,15] In the positive potential region, oxidation of Tc(III) to Tc(IV) is also observed.[1b] Each complex is characterized by a reversible Tc(III/II) redox couple, as demonstrated by the following criteria for reversibility: (i) linear plots of peak currents versus the square root of the scan rate, (ii) typical peak-to-peak separations for one-electron redox processes of inorganic complexes in nonaqueous solvents, and (iii) ratios of peak currents that are approximately unity. In contrast, the Tc(II/I) redox couple exhibits reversible behavior at 20 °C only when R is $CH_2C_6H_5$; when R is CH_3 or C_6H_5, the i_{pc}/i_{pa} ratio is greater than 1, and additional redox waves are observed on subsequent scans from electroactive reaction products that are generated from the unstable Tc^I species. This behavior is illustrated in Figure 5a by the cyclic voltammogram of *cis*-$[Tc(SC_6H_5)_2(DIARS)_2]^+$ in 0.5 M TEAP/DMF at 20 °C. In addition, a positive potential scan (Figure 5b) indicates that each complex exhibits an irreversible oxidation of Tc^{III} to Tc^{IV}. Figure 6 depicts the cyclic voltammogram after cooling to −70 °C. The rate of chemical decomposition of $[Tc(SC_6H_5)_2(DIARS)_2]^-$ is sufficiently retarded at this temperature so that reversible electrochemistry without concomitant decomposition is observed for the Tc(II/I) couple. When R = C_6H_5, the cyclic voltammogram at −70 °C shows that decomposition of the Tc(IV) species is also retarded, and thus the corresponding metal-based reduction of Tc^{IV} to Tc^{III} is observed.

The electrochemical information from spectropotentiostatic experiments[10,16,17] performed on the three $[Tc(SR)_2(DIARS)_2]^+$

Table VIII. Electrochemical Potentials for $[Tc(X)_2(DIARS)_2]^+$ Complexes in 0.5 M TEAP/DMF[a,b]

	Tc(III/II) $E°'$	Tc(II/I) $E°'$	Tc(III/IV)[c] E_{pa}
trans-$[Tc(I)_2(DIARS)_2]^+$ [d]	+0.135	−0.98	
trans-$[Tc(Br)_2(DIARS)_2]^+$ [d]	+0.020	−1.12	
trans-$[Tc(Cl)_2(DIARS)_2]^+$ [d]	−0.061	−1.26	
cis-$[Tc(SC_6H_5)_2(DIARS)_2]^+$	−0.322	−1.22	+0.94[e]
trans-$[Tc(SCH_2C_6H_5)_2(DIARS)_2]^+$	−0.362	−1.56	+1.07
trans-$[Tc(SCH_3)_2(DIARS)_2]^+$	−0.465	−1.70	+1.08[f]

[a] 20 °C; PDE working electrode; scan rate 100 mV/s. [b] $E°' = (E_{pc} + E_{pa})/2$ in V vs Ag/AgCl (3 M NaCl) from cyclic voltammetry. [c] Irreversible oxidation at 20 °C. Peak potential is reported unless otherwise noted. [d] Reference 27. Potentials are converted from the NaSCE reference electrode by addition of 30 mV. [e] Becomes chemically reversible at −70 °C. $E°'$ is reported. [f] Not well defined.

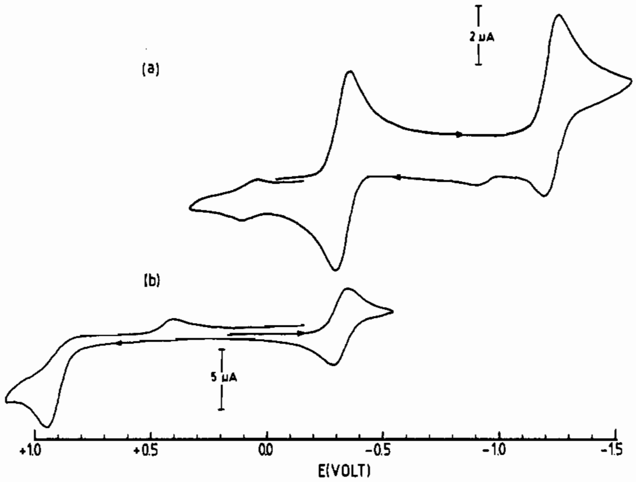

Figure 5. Cyclic voltammograms of 1.0 mM *cis*-$[Tc(SC_6H_5)_2(DIARS)_2]^+$ in 0.5 M TEAP/DMF at a PDE and 20 °C: (a) Negative potential region; (b) positive potential region. Scan rate is 100 mV/s.

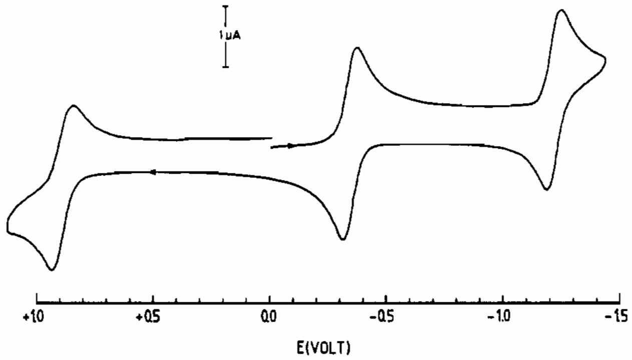

Figure 6. Cyclic voltammogram of 1.0 mM *cis*-$[Tc(SC_6H_5)_2(DIARS)_2]^+$ in 0.5 M TEAP/DMF at a PDE and −70 °C. Scan rate is 100 mV/s.

---

(15) Libson, K.; Barnett, B. L.; Deutsch, E. *Inorg. Chem.* **1983**, *22*, 1695–1704.

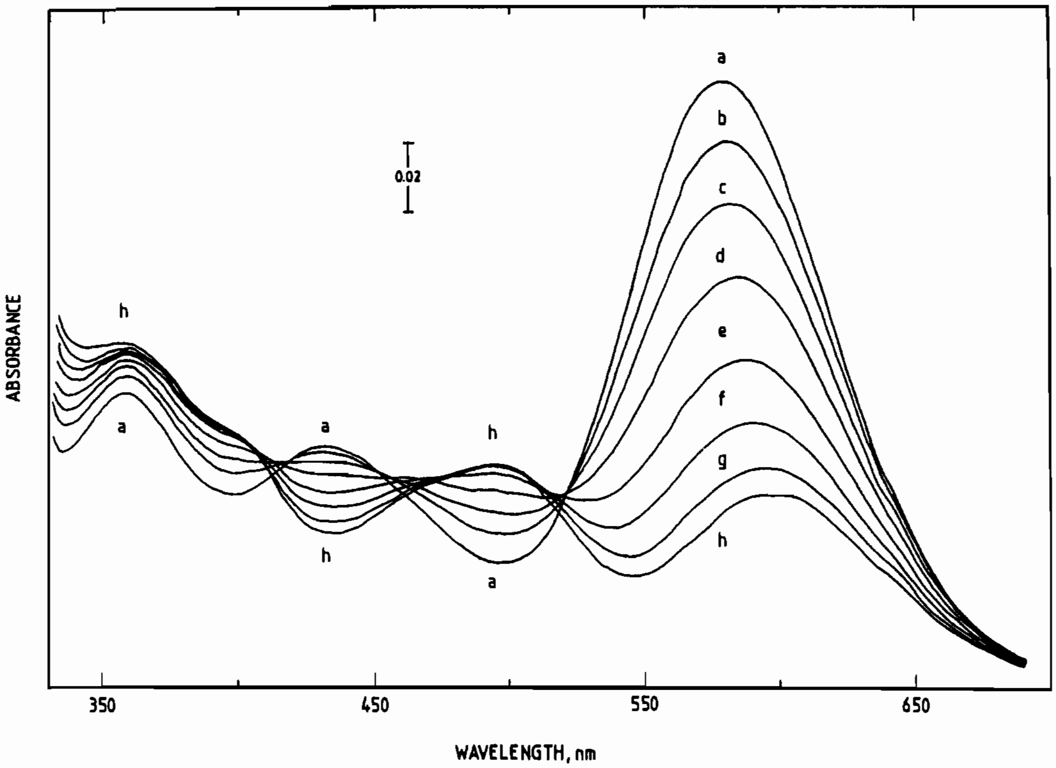

Figure 7. Sequential absorption spectra obtained during an OTTLE spectropotentiostatic experiment in 0.83 mM *cis*-$[Tc(SC_6H_5)_2(DIARS)_2]^+$ in 0.5 M TEAP/DMF. Potentials in V vs Ag/AgCl: (a) 0.000; (b) −0.260; (c) −0.280; (d) −0.300; (e) −0.320; (f) −0.340; (g) −0.370; (h) −0.600.

Table IX. Spectrophotometric Data for $[Tc(SR)_2(DIARS)_2]^+$ Complexes in 0.5 M TEAP/DMF[a]

	λ_{max}, nm	
	Tc(III)	Tc(II)
trans-$[Tc(SCH_3)_2(DIARS)_2]^{+b}$	590	533, 390 sh
trans-$[Tc(SCH_2C_6H_5)_2(DIARS)_2]^{+c}$	603	536
cis-$[Tc(SC_6H_5)_2(DIARS)_2]^{+b}$	578, 430, 356	594, 495, 464 sh, 402 sh, 360

[a] Determined by spectroelectrochemistry in an OTTLE; sh denotes a shoulder. [b] Slow decomposition (see text). [c] Rapid decomposition.

complexes was limited by their instability in 0.5 M TEAP/DMF on the longer time scale of the thin-layer experiments. The relative stabilities decrease in an order parallel to that of the alkanethiolato series,[1b] i.e., R = $CH_3 > C_6H_5 > CH_2C_6H_5$. However, all three of the thiolato–DIARS–Tc^{III} complexes have sufficient stability in this medium to allow potential step spectroelectrochemistry to be conducted in the thin-layer cell. This permitted characterization of the absorption spectra of the Tc^{III} and Tc^{II} oxidation states for each complex. These data are summarized in Table IX. The behavior of *trans*-$[Tc(SCH_3)_2(DIARS)_2]^+$ during the spectropotentiostatic experiment is identical to that observed previously for *trans*-$[Tc(SCH_3)_2(DMPE)_2]^+$,[1b] where an equilibrium of cis and trans isomers in solution is hypothesized. The spectra recorded during a thin-layer spectropotentiostatic experiment for *cis*-$[Tc(SC_6H_5)_2(DIARS)_2]^+$ are shown in Figure 7.

Discussion

Synthesis and Characterization. The Tc–DIARS complexes with thiolato ligands, $[Tc(SR)_2(DIARS)_2]^{0/+}$ (R = CH_3, $CH_2C_6H_5$, C_6H_5), can be prepared by a method similar to that used for the analogous DMPE complexes, $[Tc(SR)_2(DMPE)_2]^{0/+}$. During the preparation of $[Tc(SCH_3)_2(DIARS)_2]^+$ and $[Tc(SCH_2C_6H_5)_2(DIARS)_2]^+$, only the trans isomers were apparently formed. This is in agreement with the behavior observed for the DMPE complexes, wherein all alkane- and phenylmethanethiolates of Tc–DMPE are trans.[1b] However, the electrochemical results for both the DMPE and DIARS systems suggest that the cis isomer may be a minor component generated during the redox reactions (vide infra).

In the reaction utilizing arenethiolates, both cis and trans isomers are recognized as products with either DIARS or DMPE ligands. No interconversioin to the cis isomer was observed for the *trans*-$[Tc^{II}(SC_6H_5)_2(DIARS)_2]^0$ product, while the Tc^{III} complex showed pronounced trans → cis conversion. Thus, it can be concluded that trans → cis isomerization is faster for Tc^{III} than for Tc^{II}. This trend also has been observed[1d] for $[Tc(SC_6H_5\text{-}p\text{-}Cl)_2(DMPE)_2]^{0/+}$. The trans → cis isomerization of *trans*-$[Tc^{III}(SC_6H_5)_2(DIARS)_2]^+$ in solution is similar to, but much slower than, that observed for $[Tc(SC_6H_5\text{-}p\text{-}X)_2(DMPE)_2]^+$ (X = OCH_3, $C(CH_3)_3$, CH_3, H, Cl). After *trans*-$[Tc^{II}(SC_6H_5\text{-}p\text{-}X)_2(DMPE)_2]^0$ is oxidized to Tc^{III}, the isomerization to the cis form is so rapid that no *trans*-$[Tc^{III}(SC_6H_5\text{-}p\text{-}X)_2(DMPE)_2]^+$ product has been isolated. Also with Tc^{II}, the trans → cis isomerization is faster with DMPE ligands than with DIARS ligands (cf. $[Tc(SC_6H_4\text{-}p\text{-}Cl)_2(DMPE)_2]^0$ and $[Tc(SC_6H_5)_2(DIARS)_2]^0$). So, it can also be concluded that the trans → cis isomerization is slower for these DIARS complexes than for corresponding DMPE complexes. Overall, the present report supports an earlier generalization about $[Tc(SR)_2(D)_2]^+$ complexes: i.e., the trans form is favored when R = alkyl or benzyl, while the cis form is more stable when R = aryl.

Facile isomerization accompanies the redox reactions of Os(III/II) in phosphine–thiol complexes,[18] yielding cis Os^{II} and trans Os^{III} products. This has been rationalized on the basis of better π-back-bonding in the cis arrangement (because the good π-acceptor phosphines are competing with poor π-accepting thiols) but at the cost of some steric crowding (adjacent PPh_3 groups). In our studies of $[Tc(SR)_2D_2]^{+/0}$, we are coming to the conclusion that steric considerations are the predominant factor in directing the relative geometrical arrangement. The Tc^{III} and Tc^{II} dihalo complexes $[TcX_2D_2]^{+/0}$ are always trans with no apparent crowding. The alkanethiolato complexes $[Tc(SR)_2D_2]^{+/0}$ are also trans but at the cost of a normal tetrahedral Tc–S–R angle (vide

---

(16) Heineman, W. R. *Denki Kagaku* **1982**, *50*, 142–148.

(17) Kirchhoff, J. R.; Heineman, W. R.; Deutsch, E. *J. Pharm. Biomed. Anal.* **1986**, *4*, 777–787.

(18) Pramanik, A.; Bag, N.; Ray, D.; Lahiri, G. K.; Chakravorty, A. *Inorg. Chem.* **1991**, *30*, 410–417.

infra, the crystal structure discussion section). The analogous arenethiolato complexes assume cis geometry, apparently due to the increased steric requirements of the S–Ph group. This effect is more pronounced for Tc^{III} than for Tc^{II}, since the Tc^{III}–S bond length is shorter than the Tc^{II}–S length.

The identifiable fragments in the FAB mass spectra of these complexes can hint at comparative binding strengths. Fragment ions due to the loss of the DIARS ligand, $[Tc(SR)_2(DIARS)]^+$, are observed for *trans*-$[Tc(SCH_3)_2(DIARS)_2]^+$ as well as for *trans*-$[Tc(SCH_2C_6H_5)_2(DIARS)_2]^+$, while no fragment ion due to the loss of the DMPE ligand is observed for the analogous DMPE complexes with alkanethiolato ligands, *trans*-$[Tc(SR)_2(DMPE)_2]^+$ (R = C_3H_7, C_2H_5, CH_3, $CH_2C_6H_5$, $CH_2C_6H_4$-*p*-OCH_3). This suggests that DMPE ligands are more strongly bound to the Tc atom than are thiolato ligands but the reverse is true for DIARS complexes. It is noteworthy that no fragment ions showing a loss of the benzene group are observed for *trans*-$[Tc(SC_6H_5)_2(DIARS)_2]^+$, *cis*-$[Tc(SC_6H_5)_2(DIARS)_2]^+$, or *trans*-$[Tc(SC_6H_5)_2(DIARS)_2]^0$. Likewise, arenethiolato complexes of Tc–DMPE, *cis*-$[Tc(SC_6H_4$-*p*-$X)_2(DMPE)_2]^+$ (X = OCH_3, $C(CH_3)_3$, CH_3, H, Cl), show no fragment ions resulting from S–C bond cleavage. However, when the thiolate is alkyl-substituted, S–C bond cleavage is routinely observed in the fragmentation patterns of the mass spectra of both DMPE and DIARS ligands.

Visible–UV Spectra. The spectral transitions exhibited by Tc thiolates with DIARS ligands are generally similar to those of Tc thiolates with DMPE ligands and DEPE ligands.[1] Typically, there are two or three intense absorptions in the visible region assigned to STTCT. The UV region contains charge-transfer transitions originating on either phosphorus (DMPE) or arsenic (DIARS). Additionally, those thiolato ligands containing an aromatic moiety (e.g., $^-SCH_2C_6H_5$ or $^-SC_6H_5$) exhibit very intense ($\epsilon > 30 \times 10^3$ M^{-1} cm^{-1}) $\pi \rightarrow \pi^*$ ligand transitions, which sometimes obscure the lower intensity P/As → Tc bands.

The visible spectra for the alkane- and phenylmethanethiolato–DIARS–Tc(III) complexes, *trans*-$[Tc(SCH_3)_2(DIARS)_2]^+$ and *trans*-$[Tc(SC_6H_5)_2(DIARS)_2]^+$, are shown in Figure 1. The most prominent absorption occurs at ~17 000 cm^{-1} with a less intense peak at ~30 000 cm^{-1}. No absorption component appears between them. These two visible bands have been similarly observed in *trans*-$[Tc(SR)_2(DMPE)_2]^+$ complexes but at slightly lower energies. (Cf. for R = CH_3: 17.01 × 10^3 and 30.67 × 10^3 cm^{-1} for D = DIARS and 16.81 × 10^3 and 28.49 × 10^3 cm^{-1} for D = DMPE. Cf. also for R = $CH_2C_6H_5$: 16.64 × 10^3 and 29.50 × 10^3 cm^{-1} for D = DIARS and 16.45 × 10^3 and 27.93 × 10^3 cm^{-1} for D = DMPE.) The higher energy STTCT bands of Tc^{III}–DIARS compared to Tc^{III}–DMPE in these complexes imply a larger splitting of the t_{2g} orbital due to the Tc–DIARS π interaction. As the electrochemical results suggest below, DIARS is apparently a more effective π-acceptor in *trans*-$[Tc(S$-alkyl$)_2(DIARS)_2]^+$ than DMPE in *trans*-$[Tc(S$-alkyl$)_2(DMPE)_2]^+$. Within a particular equatorial set of ligands, either DIARS or DMPE, complexes with $^-SCH_3$ axial ligands have higher energy absorptions (by ca. 370 cm^{-1}) than those with $^-SCH_2C_6H_5$ as axial ligands, which reflects the lower nucleophilicity of sulfur in the phenylmethanethiolato ligand. These energy shifts are minor compared to the large change in the STTCT energies which is generated upon changing the Tc oxidation state. For example, the main intense visible band in $[Tc^{III}(SCH_2C_6H_5)_2(DIARS)_2]^+$ undergoes a hypsochromic shift of ca. 2000 cm^{-1} upon reduction to the Tc^{II} complex, and similar shifts have been observed in the series of alkanethiolato–DMPE–Tc complexes. The higher effective nuclear charge density of Tc^{II} causes it to be more resistant to CT from sulfur to Tc than in Tc^{III} complexes.

The trans Tc^{III} and Tc^{II} complexes with benzenethiolate, *trans*-$[Tc(SC_6H_5)_2(DIARS)_2]^{+/0}$, show a main visible absorption band at much lower energy than analogous alkane- and phenylmethanethiolato complexes. For the *trans*-$[Tc^{II}(SR)_2(DIARS)_2]^0$ series, these energies are 17.06 × 10^3 cm^{-1} for R = C_6H_5, 18.66 × 10^3 cm^{-1} for R = $CH_2C_6H_5$, and 18.76 × 10^3 cm^{-1} for R = CH_3. For the *trans*-$[Tc^{III}(SR)_2(DIARS)_2]^+$ series, this intense band is located at 14.31 × 10^3 cm^{-1} for R = C_6H_5, 16.64 × 10^3 cm^{-1} for R = $CH_2C_6H_5$, and 17.01 × 10^3 cm^{-1} for R = CH_3. The large magnitude of the bathochromic shift which occurs upon changing the alkanethiolate to an arenethiolate may be related to a partial conjugation of a suflur (3p) π-orbital to the aromatic ring[19] and supports our assignment of this higher energy STTCT as arising from a sulfur (π) → Tc (t_{2g}) charge transfer. The resistance to S–C bond cleavage observed in the mass spectra for arenethiolato complexes provides more evidence for overlap between a sulfur π-orbital and the ring π-orbital.

The cis Tc^{II} complex with benzenethiolate, *cis*-$[Tc(SC_6H_5)_2(DIARS)_2]^0$, shows STTCT bands at 16.75 × 10^3 and 20.37 × 10^3 cm^{-1} and a shoulder at 25.58 × 10^3 cm^{-1}. Although this isomer could not be isolated, the extinction coefficients of these bands are estimated as (3–5) × 10^3 M^{-1} cm^{-1} from the spectrum obtained upon reduction of *cis*-$[Tc(SC_6H_5)_2(DIARS)_2]^+$. These absorptions are similar to those observed for *cis*-$[Tc(SC_6H_5$-*p*-$Cl)_2(DMPE)_2]^0$ though the STTCT bands for *cis*-$[Tc(SC_6H_5$-*p*-$Cl)_2(DMPE)_2]^0$ occur at lower energy (maxima at 16.4 × 10^3 cm^{-1} ($\epsilon = 3 \times 10^3$ M^{-1} cm^{-1}), 19.5 × 10^3 cm^{-1} ($\epsilon = 3 \times 10^3$ M^{-1} cm^{-1}), and 22.0 × 10^3 cm^{-1} ($\epsilon = 4 \times 10^3$ M^{-1} cm^{-1})).

Crystal Structures. The molecular structures reported herein for $[Tc(SCH_3)_2(DIARS)_2]^+$ (**1**) and $[Tc(SC_6H_5)_2(DIARS)_2]^0$ (**2**) comprise comparable trans complexes. A number of related bis(thiolato)–technetium–phosphine complexes have had their structural parameters tabulated.[1d] This tabulation clearly shows Tc–S bond lengths to be dependent on the Tc oxidation state with average lengths of Tc^{III}–S = 2.297 (6) Å and Tc^{II}–S = 2.424 (3) Å. Thus, the Tc–S distance contracts ca. 0.13 Å upon oxidation from Tc^{II} to Tc^{III}. Further, this difference occurs regardless of the geometry (cis/trans) or whether the thiolato ligand is alkyl or aryl substituted. The DIARS complexes, **1**, **2**, agree well with these previous observations. The Tc^{III}–$S(CH_3)$ length in **1** is 2.292 (2) Å and the Tc^{II}–$S(C_6H_5)$ length in **2** is 2.410 (2) Å. Thus the magnitudes of the Tc–S lengths seem to be largely unrelated to whether phosphine or arsine ligands are present. The decreasing Tc–S bond length with increasing Tc oxidation state is behavior associated with σ-donation as the primary mode of ligand–metal bonding. The difference in Tc–S between the two DIARS structures of ca. 0.12 Å is nearly the same as that for related DMPE structures, so we conclude that the Tc–S bonding in the presence of arsine ligands is very similar to that observed in the presence of phosphine ligands.

In complex **1**, the important structural parameters in the methanethiolato ligand are S–CH_3 = 1.816 (7) Å and Tc–S–CH_3 = 118.9°. Both the bond distance and bond angle are slightly smaller than those observed for the very similar complexes, *trans*-$[Tc(SCH_3)_2(D)_2]^+$, D = DMPE (1.842 (7) Å and 122.3 (8)°) and D = DEPE (1.821 (4) Å and 121.2 (1)°).[1a] In complex **2**, S–C_6H_5 = 1.794 (7) Å and Tc–S–C_6H_5 = 119.5 (3)°. For comparison, the related complex *cis*-$[Tc(SC_6H_5)_2(DMPE)_2]^+$ shows S–C = 1.77 (2) Å and Tc–S–C = 118.5 (6)°. Two pertinent generalizations that arise from Tc–DMPE[1d] structural data are that (i) *trans*-$[Tc(SR)_2(D)_2]^{0/+}$ complexes have Tc–S–C angles greater than 120°, while similar cis complexes have Tc–S–C angles less than 120°, and (ii) S–C(alkyl) ranges from 1.82 to 1.84 Å for $[Tc(SR)_2(D)_2]^{0/+}$ complexes, while the S–C(aryl) range is smaller, at 1.76–1.78 Å. Steric interactions seem to be the significant factor in the larger Tc–S–C angles for the trans complexes. Hybridization at the carbon atom accounts for the different S–C lengths. The DIARS structures, **1** and **2**, are in close agreement with these generalizations regarding geometry about the thiolato S atom.

The Tc–As bond lengths average 2.496 (2) Å in **1** and 2.471 (2) Å in **2**. The difference is 0.025 Å between the two complexes, with the longer length associated with the higher Tc oxidation state. This behavior parallels that of Tc–P bond lengths in Tc^{II} and Tc^{III} complexes with diphosphine ligands and is indicative of π-back-bonding interactions. Only two other Tc–DIARS structures have been reported, $[Tc(DIARS)_2Cl_2]^+$ and [Tc-

---

[19] Blower, P. J.; Dilworth, J. R. *Coord. Chem. Rev.* **1987**, *76*, 121–185.

$(DIARS)_2Cl_4]^+$. In $[Tc^{III}(DIARS)_2Cl_2]^+$, the Tc–As length averages 2.512 (5) Å,[20] which is close to the Tc^{III}–As length in **1**. The Tc–As distance in the 8-coordinate Tc^V complex, $[Tc^V(DIARS)_2Cl_4]^+$, is naturally longer, at 2.578 (2) Å.[21]

While **1** has longer Tc–As lengths than structure **2**, it has shorter As–C lengths on average. The average As–C length is ca. 0.02 Å shorter in **1** than in **2** for both As–C(methyl) and As–C(phenylene). It is reasonable to suspect that more effective overlap of As with Tc has a detrimental effect on As–C bonds. The DIARS ligand generally shows some bending between the phenyl plane and the MAs_2 coordination plane. The value of this dihedral angle is quite a flexible parameter. Skelton and White[22] list several metal–DIARS examples that show bending angles ranging from 2.7 to 28°. The bends in the DIARS ligands reported herein are 10.6 (4) and 2.0 (6)° for **1** and **2**, respectively. Other common characteristics of the DIARS ligand include a distortion of the bond angles about As such that all C–As–C angles are less than the ideal tetrahedral value and all M–As–C(methyl) angles are greater than the tetrahedral value. This results in the methyl groups on As bending away from the metal center and has been postulated as being a consequence of s-character in bonding within the free DIARS molecule.[22-24] Also common is the asymmetric placement of methyl groups on As relative to the basal coordination plane and/or the phenylene plane.[25] These features are also evident in the title structures.

Electrochemistry. The electrochemical behavior of this series of $[Tc(SR)_2(DIARS)_2]^+$ complexes is qualitatively similar to that which has been described for the related series of *trans*-$[MX_2D_2]^+$ (M = Tc, Re; X = Cl, Br; D = DIARS, DMPE),[8,15,26,27] *trans*-$[Tc(SR)_2(DMPE)_2]^+$ (SR = alkanethiolato ligand),[1a,b] and *cis*-$[Tc(SR)_2(DMPE)_2]^+$ (SR = arenethiolato ligand)[1d] complexes. The redox behavior is characterized by a reversible M(III/II) couple and related M(II/I) and M(IV/III) couples which exhibit varying degrees of reversibility depending on the nature of X and D and on the solution temperature. The data of Table VIII indicate that the $[Tc(SR)_2(DIARS)_2]^+$ complexes, as was the case with the thiolato–DMPE–Tc^{III} complexes, are several hundred millivolts more difficult to reduce than the corresponding dihalo–Tc^{III} analogues, which attests to the strong σ-donating ability of the thiolato ligands.[1b]

The unique thiolato–DIARS–Tc^{III} series allows several assessments of the subtle effects of the ligand environment (i.e., SR and D variations) on the $E^{\circ\prime}$ values of the Tc(III/II) and Tc(II/I) redox couples. A cross-series comparison of the three thiolato–DIARS complexes to the analogous thiolato–DMPE complexes indicates that when the thiolato ligand is SCH_3 or $SCH_2C_6H_5$, the $E^{\circ\prime}$ values of the thiolato–DIARS analogues shift to more positive potentials (shift = 85 mV for methanethiolato and 151 mV for phenylmethanethiolato). This effect is consistent with the additional π-acid character within the framework of the DIARS backbone. Enhanced π-acid character from pendant aryl substituents on D, as well as within the D ligand backbone, has previously been observed to result in a positive shift in $E^{\circ\prime}$.[15,26,28] In contrast, a comparison of reduction potentials for the arenethiolato complexes, *cis*-$[Tc(SC_6H_5)_2(DMPE)_2]^+$ and *cis*-$[Tc(SC_6H_5)_2(DIARS)_2]^+$, show a shift of −23 mV; i.e., the DMPE complex is easier to reduce. This situation presumably results from the cis geometry, wherein the DMPE ligand is better able to function as a π-acid, due to the rigidity of the DIARS ligand. Within the DIARS series, potential shifts are observed for changes in SR which parallel the nucleophilic character at sulfur. SCH_3 exhibits the most negative $E^{\circ\prime}$ value, and as the SR ligand is modified with substituents that enhance the π-acid character of the ligand ($SCH_2C_6H_5$ and SC_6H_5), the $E^{\circ\prime}$ becomes more positive with the greatest shift occurring between alkyl and aryl substituents. A recent study[29] of *trans*-$[Re(SR)_2D_2]^+$ reduction potentials has found the same ordering for Re(III/II); i.e., $E^{\circ\prime}$ increases in the order $SC_2H_5 < SCH_2C_6H_4$-*p*-$OCH_3 < SCH_2C_6H_5 < SC_6H_4$-*p*-$CH_3 < SC_6H_5 < SC_6H_4$-*p*-Cl, although these Re^{III} complexes are ca. 270 mV more difficult to reduce than Tc^{III} analogues. Interestingly for the $[Re(SR)_2D_2]^+$ complexes reported, only the trans isomer has been observed.

The potential difference between the Tc(III/II) and Tc(II/I) redox couples is 900 mV when SR is SC_6H_5 and 1200 mV when SR is SCH_3 and $SCH_2C_6H_5$. These potential differences are consistent with those observed for the thiolato–DMPE–Tc^{III} series; the magnitude of each difference presumably reflects differences in sulfur nucleophilicity toward the metal center.[1d]

Spectroelectrochemistry. The instability of *trans*-$[Tc(SCH_2C_6H_5)_2(DIARS)_2]^+$ in 0.5 M TEAP/DMF limits the characterization of the Tc^{III} and Tc^{II} species to potential step spectroelectrochemistry. In addition to the characteristic Tc^{III} and Tc^{II} STTCT bands listed in Table IX, an additional peak common to both oxidation states is observed at 465 nm. The peak grows with time and does not change as a function of the potential step. Presumably, this absorption originates in a species that is the result of decomposition of the Tc^{III} parent complex and is not electroactive in the range of the potential step, since evidence of a new species in the thin-layer voltammogram is not observed. Decomposition also occurs in the spectroelectrochemical study of *cis*-$[Tc(SC_6H_5)_2(DIARS)_2]^+$ although not to the same extent as for *trans*-$[Tc(SCH_2C_6H_5)_2(DIARS)_2]^+$. Spectrum a in Figure 7 depicts the absorption of *cis*-$[Tc(SC_6H_5)_2(DIARS)_2]^+$, while spectrum h represents the absorption spectrum of the reduced complex, *cis*-$[Tc(SC_6H_5)_2(DIARS)_2]^0$. Retention of the cis geometry for both the Tc^{II} and Tc^{III} complexes is established during the spectroelectrochemistry experiment by a comparison of spectra a and h to those obtained during analogous experiments on the previously studied cis thiolato–DMPE–Tc^{III} complexes.[1b] The isosbestic points in Figure 7 gradually shift during the spectroelectrochemistry experiment. This indicates that slow decomposition occurs. The occurrence of such decomposition is supported by a chronoabsorptometry experiment, which demonstrates (a) only 83% absorbance regeneration after the spectropotentiostatic reduction and (b) the appearance of a shoulder at 464 nm. The shoulder at 464 nm is similar to the additional peak observed in the Tc^{III} and Tc^{II} spectra when SR is $SCH_2C_6H_5$. No new electrochemical processes are observed in the thin-layer cyclic voltammogram after spectropotentiostatic reduction.

The methanethiolato–DIARS derivative exhibits thin-layer electrochemical and spectroelectrochemical behavior similar to that of the DMPE congener, although chronoabsorptometry and a shift in the isosbestic point indicate a decomposition pathway may also be present. In the DMPE case, a cis/trans equilibrium was hypothesized to exist in solution.[1b]

Summary

The complexes $[Tc(SR)_2(DIARS)_2]^+$ with R = CH_3, $CH_2C_6H_5$, and C_6H_5 have been prepared and their properties compared with those of the analogous diphosphine complexes $[Tc(SR)_2(DMPE)_2]^+$. When SR is an alkanethiolate or phenylmethanethiolate, the trans isomer is formed. Both cis and trans isomers are obtained for SR = benzenethiolate although the cis isomer is more stable. Trans → cis isomerization proceeds more slowly for $[Tc(SC_6H_5)_2(DIARS)_2]^+$ than for $[Tc(SC_6H_5)_2(DMPE)_2]^+$. An examination of FAB mass spectral fragments implies that Tc–P

---

(20) Elder, R. C.; Whittle, R.; Glavan, K. A.; Johnson, J. F.; Deutsch, E. *Acta Crystallogr.* **1980**, *B36*, 1662–1665.

(21) Glavan, K. A.; Whittle, R.; Johnson, J. F.; Elder, R. C.; Deutsch, E. *J. Am. Chem. Soc.* **1980**, *102*, 2103–2104.

(22) Skelton, B. W.; White, A. H. *J. Chem. Soc., Dalton Trans.* **1980**, 1556–1566.

(23) Pauling, P. J.; Porter, D. W.; Robertson, G. B. *J. Chem. Soc. A* **1970**, 2728–2731.

(24) Drew, M. G. B.; Wilkins, J. D. *J. Chem. Soc., Dalton Trans.* **1973**, 2664–2669.

(25) Salah, O. M. A.; Bruce, M. I.; Lohmeyer, P. J.; Raston, C. L.; Skelton, B. W.; White, A. H. *J. Chem. Soc., Dalton Trans.* **1981**, 962–967.

(26) Kirchhoff, J. R.; Heineman, W. R.; Deutsch, E. *Inorg. Chem.* **1987**, *26*, 3108–3113.

(27) Hurst, R. W.; Heineman, W. R.; Deutsch, E. *Inorg. Chem.* **1981**, *20*, 3298–3303.

(28) Wilcox, B. E.; Deutsch, E. *Inorg. Chem.* **1991**, *30*, 688–693.

(29) Chang, L.; Aizawa, S.-I.; Heeg, M. J.; Deutsch, E. *Inorg. Chem.* **1991**, *30*, 4920–4927.

in $[Tc(SR)_2(DMPE)_2]^+$ is bound more strongly than Tc–As in $[Tc(SR)_2(DIARS)_2]^+$.

Tc–S bond lengths of 2.29 Å for Tc^{III} and 2.41 Å for Tc^{II} have been observed for *trans*-$[Tc(SR)_2(DIARS)_2]^{+/0}$ and are equivalent to those observed for $[Tc(SR)_2(DMPE)_2]^{+/0}$. The contraction of Tc–As with decreasing Tc oxidation state indicates significant π-character in this bond.

The absorption spectra of *trans*-$[Tc(S\text{–}alkyl)_2(DIARS)_2]^+$ show two intense visible bands which correspond to, but are higher in energy than, those of *trans*-$[Tc(S\text{–}alkyl)_2(DMPE)_2]^+$ and are assigned as S → Tc CT transitions. *cis*-$[Tc(S\text{–}aryl)_2(DIARS)_2]^+$ possesses three intense visible bands which are again assigned to S → Tc transitions and which are similar to those observed in the analogous DMPE system. The UV region is populated by As → Tc CT bands and $\pi \rightarrow \pi^*$ ligand transitions when the sulfur substituent is aromatic.

All of the *trans*-$[TcX_2(DIARS)_2]^{+/0}$ complexes we have examined (X = Cl, Br, SCH_3, $SCH_2C_6H_5$) are easier to reduce than their DMPE congeners, with differences in $E^{\circ\prime}$ values ranging from 85 to 170 mV (Tc(III/II)) and from 20 to 150 mV (Tc(II/I)). However, *cis*-$[Tc(SC_6H_5)_2(DIARS)_2]^{+/0}$ is 23 mV (Tc(III/II)) and 110 mV (Tc(II/I)) more difficult to reduce than *cis*-$[Tc(SC_6H_5)_2(DMPE)_2]^{+/0}$.

The spectroscopic and electrochemical results together suggest that, in these *trans*-$[Tc(S\text{–}alkyl)_2D_2]^+$ complexes, DIARS is a more effective π-acceptor than DMPE. The origin of this enhanced π-acidity seems to be the aromatic backbone in DIARS. However, for the *cis*-$[Tc(S\text{–}aryl)_2D_2]^+$ complexes DIARS is a poorer π-acceptor than DMPE, presumably due to the rigidity of the DIARS ligand and its implications for M–L $d\pi$–$p\pi$ overlap in the cis configuration.

Acknowledgment. Financial support by the National Institutes of Health (Grants HL-21276 and CA-42179 (E.D.)), by the Department of Energy (Grant DE-FG02-86ER60487 (W.R.H.)), and by Mallinckrodt, Inc. (E.D.), is gratefully acknowledged. The diffractometer used herein was purchased through an NSF equipment grant to Wayne State University.

Registry No. 1, 139168-01-7; **2**, 129370-83-8; *trans*-$[^{99}Tc(OH)(O)(DIARS)_2](PF_6)_2$, 139168-00-6; *trans*-$[^{99}Tc(SCH_2C_6H_5)_2(DIARS)_2]PF_6$, 139168-02-8; *trans*-$[^{99}Tc^{II}(SCH_2C_6H_5)_2(DIARS)_2]^0$, 129370-77-0; *cis*-$[^{99}Tc^{II}(SC_6H_5)_2(DIARS)_2]^0$, 139240-61-2; *cis*-$[^{99}Tc(SC_6H_5)_2(DIARS)_2]PF_6$, 139240-63-4; *trans*-$[^{99}Tc(SC_6H_5)_2(DIARS)_2]PF_6$, 139168-03-9; *trans*-$[^{99}Tc^{II}(SCH_3)_2(DIARS)_2]^0$, 129423-99-0; *cis*-$[^{99}Tc^{IV}(SC_6H_5)_2(DIARS)_2]^{2+}$, 139168-04-0; *trans*-$[^{99}Tc^{I}(SCH_2C_6H_5)_2(DIARS)_2]^-$, 139168-05-1; $NH_4{}^{99}TcO_4$, 34035-97-7.

Supplementary Material Available: For *trans*-$[Tc(SCH_3)_2(DIARS)_2]PF_6$ and *trans*-$[Tc(SC_6H_5)_2(DIARS)_2]$, Tables A, C–F, and H–K, containing experimental crystallographic data, complete bond lengths and angles, thermal parameters, hydrogen parameters, and least-squares planes (9 pages); Tables B and G, listing calculated and observed structure factors (44 pages). Ordering information is given on any current masthead page.

Contribution from the Department of Chemistry, University of Calgary, Calgary, Alberta T2N 1N4, Canada, and University of British Columbia, Vancouver, British Columbia V6T 1Y6, Canada

Characterization of the $GaO_4Al_{12}(OH)_{24}(H_2O)_{12}{}^{7+}$ Polyoxocation by MAS NMR and Infrared Spectroscopies and Powder X-ray Diffraction

Susan M. Bradley,[†] Ronald A. Kydd,[*,†] and Colin A. Fyfe[‡]

Received June 19, 1991

Powder X-ray diffraction studies of the selenate salts of the $GaO_4Al_{12}(OH)_{24}(H_2O)_{12}{}^{7+}$ polyoxocation ($GaAl_{12}$) have confirmed unambiguously that it is structurally analogous to the $AlO_4Al_{12}(OH)_{24}(H_2O)_{12}{}^{7+}$ species (Al_{13}). Lines in the solid-state MAS NMR spectra of $GaAl_{12}$, in which a gallium rather than an aluminum atom sits in the central tetrahedral position, are much sharper than those for the Al_{13} species. At least in part, this is because the $GaAl_{12}$ structure is less distorted than the Al_{13} ion. Line widths in the solution phase NMR spectra of the Al_{13} ion (and perhaps the $GaAl_{12}$ ion) are also affected by exchange broadening. Changes in the infrared spectra between ca. 900 and 400 cm^{-1} which result from replacing the central tetrahedral aluminum in Al_{13} with gallium, thereby forming $GaAl_{12}$, and also the changes which occur upon deuteration have been studied, and an assignment of the bands in this region has been proposed.

Introduction

The development of new types of microporous solids through the intercalation of charged metal polymers by various types of layered inorganic solids[1–5] has led to an increased interest in the types of oligomers formed upon the base hydrolysis of metal ions in solution. Our work in this area has concentrated thus far on the study of the base hydrolyses of aqueous aluminum, gallium, and mixed gallium–aluminum solutions.[6–8] It is well-known that the base hydrolysis of aqueous Al^{3+} solutions results in the formation, among other species, of the tridecameric $AlO_4Al_{12}(OH)_{24}(H_2O)_{12}{}^{7+}$ cation (i.e. Al_{13}).[9] This Al_{13} ion consists of a central tetrahedral aluminum surrounded by 12 edge-linked octahedrally coordinated aluminums,[9] arranged in an analogous fashion to the Baker–Figgis ϵ-isomer[10] of the well-known Keggin structure (the Baker–Figgis α-isomer) which occurs in the heteropoly oxometalates.[11–13] Our previous results have indicated that, upon base hydrolysis, aqueous Ga^{3+} solutions form, among other species, a $GaO_4Ga_{12}(OH)_{24}(H_2O)_{12}{}^{7+}$ unit (i.e. Ga_{13}), which appears to be isostructural with the Al_{13} species. In addition, our study of the base hydrolysis of gallium and aluminum solutions mixed in a 1:12 ratio[8] supported the previous suggestion made by Thomas et al.,[14] on the basis of a single NMR peak, that a $GaO_4Al_{12}(OH)_{24}(H_2O)_{12}{}^{7+}$ ion (i.e. $GaAl_{12}$) could be formed. While the size of this $GaAl_{12}$ species appears to be similar to that of the Al_{13} ion, its exact structure has yet to be determined.

[†] University of Calgary.

[‡] University of British Columbia.

(1) Figueras, F. *Catal. Rev.—Sci. Eng.* **1988**, *30*, 457.

(2) Sakurai, H.; Urabe, K.; Izumi, Y. *J. Chem. Soc., Chem. Commun.* **1988**, 1519.

(3) Clearfield, A.; Roberts, B. D. *Inorg. Chem.* **1988**, *27*, 3237.

(4) Olivera-Pastor, P.; Jimenez-Lopez, A.; Maireles-Torres, P.; Rodriguez-Castellon, E.; Tomlinson, A. A. G.; Alagna, L. *J. Chem. Soc., Chem. Commun.* **1989**, 751.

(5) Cheng, S.; Wang, T.-C. *Inorg. Chem.* **1989**, *29*, 1283.

(6) Bradley, S. M.; Kydd, R. A.; Yamdagni, R. *J. Chem. Soc., Dalton Trans.* **1990**, 413.

(7) Bradley, S. M.; Kydd, R. A.; Yamdagni, R. *J. Chem. Soc., Dalton Trans.* **1990**, 2653.

(8) Bradley, S. M.; Kydd, R. A.; Yamdagni, R. *Magn. Reson. Chem.* **1990**, *28*, 746.

(9) Johansson, G. *Ark. Kemi.* **1963**, *20*, 321.

(10) Baker, L. C. W. and Figgis, J. S. *J. Am. Chem. Soc.* **1970**, *92*, 3794.

(11) Keggin, J. F. *Nature* **1933**, *131*, 908.

(12) Keggin, J. F. *Proc. R. Soc. London, A* **1934**, *144*, 75.

(13) Pope, M. T. *Heteropoly and Isopoly Oxometalates*; Springer-Verlag: New York, 1983; p 27.

(14) Thomas, B.; Görz, H.; Schönherr, S. *Z. Chem.* **1987**, *27*, 183.

0020-1669/92/1331-1181$03.00/0 © 1992 American Chemical Society